The electroweak contributions to $(g-2)_\mu$ after the Higgs boson mass measurement

C. Gnendiger, D. Stöckinger, H. Stöckinger-Kim

Institut für Kern- und Teilchenphysik, TU Dresden, Dresden, Germany

Abstract

The Higgs boson mass used to be the only unknown input parameter of the electroweak contributions to $(g-2)_\mu$ in the Standard Model. It enters at the two-loop level in diagrams with e.g. top loops, W- or Z-exchange. We re-evaluate these contributions, providing analytic expressions and exact numerical results for the Higgs boson mass recently measured at the LHC. Our final result for the full Standard Model electroweak contributions is $(153.6 \pm 1.0) \times 10^{-11}$, where the remaining theory error comes from unknown three-loop contributions and hadronic uncertainties.

The anomalous magnetic moment $a_\mu = (g-2)_\mu/2$ of the muon has been measured very precisely at Brookhaven National Laboratory, with the final value [1][1]:

$$a_\mu^{\text{exp}} = (116\,592\,089 \pm 63) \times 10^{-11}\,. \tag{1}$$

This measurement has already reached a sensitivity to details of the weak interactions, which contribute at the order 10^{-9}. Future experiments planned at Fermilab [2] and J-PARC [3] aim to further reduce the uncertainty by a factor 4.

The Standard Model theory prediction has also been continuously improving, see Refs. [4, 5] for recent reviews and references. The 5-loop QED contribution has been completely calculated [6]. The hadronic vacuum polarization contributions make use of the most recent experimental data on the $(e^+ e^- \to \text{hadrons})$ cross section [7–9], and an earlier discrepancy to analyses based on τ-decays has been resolved [9, 10]. The latest results of various groups for the hadronic light-by-light contributions agree within the quoted errors [4, 11], and new non-perturbative approaches promise further progress [12, 13].

---

[1] The change in the number compared to Ref. [1] is due to a new PDG value for the magnetic moment ratio of the muon to proton, see e.g. Ref. [2]

Here we focus on the electroweak contributions to $(g-2)_\mu$ in the Standard Model. They include contributions from the Higgs boson and are the only ones which depend on the Higgs boson mass M_H. This quantity used to be the only unknown input parameter of the Standard Model, resulting in the dominant remaining theory uncertainty of the electroweak contributions. As a reference, the seminal evaluation of Ref. [14] obtained the result

$$a_\mu^{\mathrm{EW}} = (154 \pm 1 \pm 2) \times 10^{-11}, \tag{2}$$

where the first error is due to hadronic uncertainties, but the second is due to the unknown Higgs boson mass.

Now, the Higgs boson mass has been measured at the LHC to be $M_H = 125.5 \pm 0.2(\mathrm{stat.})^{+0.5}_{-0.6}(\mathrm{syst.})$ GeV by ATLAS [15] and $M_H = 125.7 \pm 0.3(\mathrm{stat.}) \pm 0.3(\mathrm{syst.})$ GeV by CMS [16]. In the following we take the average central value and a conservative error band, covering the 2σ range of both measurements:

$$M_H = 125.6 \pm 1.5 \text{ GeV.} \tag{3}$$

Given this progress on all fronts regarding $(g-2)_\mu$ and the Higgs boson it is appropriate to update the prediction of the electroweak contributions to $(g-2)_\mu$.

In the present paper we therefore re-evaluate the electroweak Standard Model contributions at the two-loop level, making use of the LHC result. We provide the full M_H-dependent part in numerical and, where not readily available, in analytical form. This allows us to obtain the exact $(g-2)_\mu$ prediction for the measured value of M_H, and to compare with previously published results and error estimates. We combine this with the most advanced computations of all other electroweak contributions up to leading 3-loop order and provide the final result and a complete discussion of the remaining theory error.

In the following our input parameters besides Eq. (3) are [17]:

$$M_W = 80.385 \pm 0.015 \text{ GeV}, \qquad m_\mu = 105.6583715 \pm 0.0000035 \text{ MeV}, \tag{4a}$$
$$M_Z = 91.1876 \pm 0.0021 \text{ GeV}, \qquad m_t = 173.5 \pm 0.6 \pm 0.8 \text{ GeV} \tag{4b}$$

for the masses of W-boson, muon, Z-boson and top quark, and

$$G_F = (1.166\,378\,7 \pm 0.000\,000\,6) \times 10^{-5} \text{ GeV}^{-2}, \quad \alpha = 1/137.035\,999 \tag{5}$$

for the muon decay constant and the fine-structure constant.

The Standard Model electroweak contributions are split up into one-loop, two-loop and higher orders as

$$a_\mu^{\mathrm{EW}} = a_\mu^{\mathrm{EW}(1)} + a_{\mu;\mathrm{bos}}^{\mathrm{EW}(2)} + a_{\mu;\mathrm{ferm}}^{\mathrm{EW}(2)} + a_\mu^{\mathrm{EW}(\geq 3)}, \tag{6}$$

where the two-loop contributions are further split into bosonic and fermionic contributions, as discussed below.

The one-loop contribution is given by [4, 5]

$$a_\mu^{\mathrm{EW}(1)} = \frac{G_F}{\sqrt{2}} \frac{m_\mu^2}{8\pi^2} \left[\frac{5}{3} + \frac{1}{3}(1 - 4s_W^2)^2 \right] = (194.81 \pm 0.01) \times 10^{-11}, \tag{7}$$
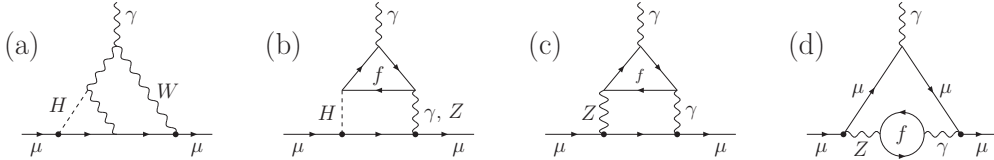
Figure 1: Sample two-loop diagrams: Higgs-dependent bosonic (a) and fermionic (b) diagram, diagram with $\gamma\gamma Z$-fermion triangle (c) and γ–Z mixing (d).

where $s_W^2 = 1 - M_W^2/M_Z^2$ is the square of the weak mixing angle in the on-shell renormalization scheme. One-loop contributions suppressed by m_μ^2/M_Z^2 or m_μ^2/M_H^2 are smaller than 10^{-13} and hence neglected here. The parametrization in terms of G_F already absorbs important higher-order contributions. The error in Eq. (7) is due to the uncertainty of the input parameters, in particular of the W-boson mass.

Before discussing higher-order contributions we briefly explain possible parametrizations in terms of G_F and α. The one-loop contribution in Eq. (7) has been parametrized in terms of G_F. Generally, n-loop contributions are proportional to $G_F \, \alpha^{(n-1)}$, and it is possible to reparametrize α in terms of other quantities. Possibilities are to replace α by a running α at the scale of the muon mass or the Z-boson mass, or to replace $\alpha \to \alpha(G_F)$, where $\alpha(G_F) \equiv \sqrt{2}G_F s_W^2 M_W^2/\pi = \alpha \times (1+\Delta r)$. The quantity Δr summarizes radiative corrections to muon decay. Different choices amount to differences which are formally of the order $n+1$. We will always choose α in the Thomson limit, i.e. given by Eq. (5).

We now turn to the first set of contributions with noticeable dependence on the Higgs boson mass: the bosonic two-loop contributions $a_{\mu;\mathrm{bos}}^{\mathrm{EW}(2)}$. They are defined by two-loop and associated counterterm diagrams without a closed fermion loop, see Fig. 1(a) for a sample diagram. They are conceptually straightforward but involve many diagrams. Their first full computation in Ref. [18] was a milestone — the first full computation of a Standard Model observable at the two-loop level. Actually, Ref. [18] employed an approximation assuming $M_H \gg M_W$. Ref. [19] confirmed the result but provided the full M_H-dependence; Ref. [20] then published the result in semianalytical form.

Here we re-evaluate the bosonic two-loop contributions using the parametrization discussed above, in terms of $G_F \alpha$. Fig. 2 shows the result for a range of Higgs boson masses. The numerical result differs by around 3% from the one given in Ref. [19], where the $G_F \, \alpha(G_F)$ parametrization was chosen. The measured value of M_H now fixes the value of these contributions and we obtain

$$a_{\mu;\mathrm{bos}}^{\mathrm{EW}(2)} = (-19.98 \pm 0.03) \times 10^{-11}. \tag{8}$$

Here the remaining parametric uncertainty results from the experimental uncertainties of the input parameters M_H, and to a smaller extent of M_W, see the right plot in Fig. 2. The result lies within the intervals given in the original
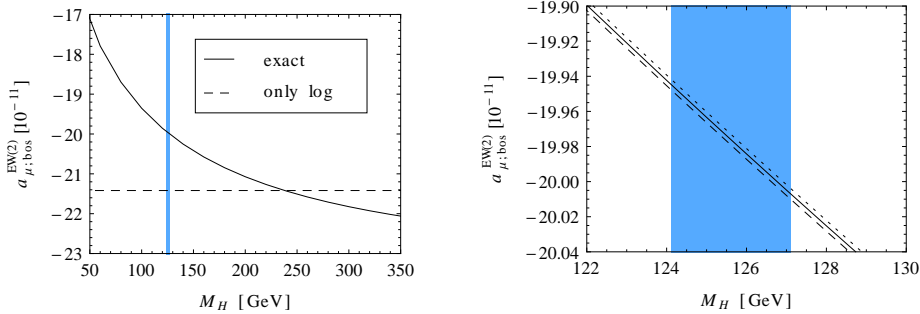
Figure 2: Numerical result for $a_{\mu;\text{bos}}^{\text{EW}(2)}$ as a function of the Higgs boson mass. The vertical band indicates the measured value of M_H. The dashed line in the left plot corresponds to the leading logarithmic approximation as defined in Ref. [19]. In the right plot the dotted, solid, dashed lines correspond to a variation of M_W by $(-15, 0, +15)$ MeV, respectively.

Refs. [19, 20] and the recent reviews [4, 5], which all differ slightly because of the different Higgs boson mass ranges and central values used for the evaluations.

The fermionic two-loop contributions $a_{\mu;\text{ferm}}^{\text{EW}(2)}$ are defined by Feynman diagrams with a closed fermion loop. The Higgs boson enters through diagrams of the type of Fig. 1(b), where a fermion loop generates a $H\gamma\gamma$ or $H\gamma Z$ interaction. The fermionic contributions involve also light quark loops, e.g. in the diagrams of Fig. 1(c), for which perturbation theory is questionable. Hence we split up these contributions further, slightly extending the notation of Ref. [5]:

$$a_{\mu;\text{ferm}}^{\text{EW}(2)} = a_{\mu}^{\text{EW}(2)}(e, \mu, u, c, d, s) + a_{\mu}^{\text{EW}(2)}(\tau, t, b) + a_{\mu;\text{f-rest,H}}^{\text{EW}(2)} + a_{\mu;\text{f-rest,no H}}^{\text{EW}(2)}. \quad (9)$$

Here the first two terms on the r.h.s. denote contributions from the diagrams of Fig. 1(c) with a $\gamma\gamma Z$-subdiagram and the indicated fermions in the loop. The third term denotes the Higgs-dependent diagrams of Fig. 1(b); the fourth collects all remaining fermionic contributions, e.g. from W-boson exchange or from diagram Fig. 1(d).

We first focus on the Higgs-dependent part, for which we write

$$a_{\mu;\text{f-rest,H}}^{\text{EW}(2)} = \sum_f \left[a_{\mu;\text{f-rest,H}\gamma}^{\text{EW}(2)}(f) + a_{\mu;\text{f-rest,HZ}}^{\text{EW}(2)}(f) \right], \quad (10)$$

where the two terms in the sum denote the Higgs-dependent diagrams of Fig. 1(b) with either a photon or a Z-boson in the outer loop and the sum extends over the Standard Model fermions; the relevant ones are $f = t, b, c, \tau$. Contributions from the remaining Standard Model fermions are below 10^{-14} and thus negligible.

The first full computation of the fermionic contributions, including the Higgs dependence was carried out in Ref. [21]. There, the dependence on the Higgs boson mass is provided in three limiting cases, $M_H \ll m_t$, $M_H = m_t$, $M_H \gg m_t$.

4

Furthermore, since $s_W^2 \approx 1/4$, terms suppressed by a factor $(1 - 4s_W^2)$, in particular the entire Higgs–Z diagrams of Fig. 1(b) were neglected. Diagrams similar to Fig. 1(b) have also been evaluated in the more complicated case of extended models, e.g. in the Two-Higgs-doublet model and the supersymmetric Standard Model [22, 23].

We computed the Higgs-dependent diagrams without approximations in two ways: with the technique developed for Ref. [19,24] using asymptotic expansion and integral reduction techniques, and with the method of Barr and Zee, where the inner loop is computed first and then inserted into the outer loop [25]. The result from this is

$$a_{\mu;\text{f-rest,H}\gamma}^{\text{EW(2)}}(f) = \frac{G_F}{\sqrt{2}} \frac{m_\mu^2}{8\pi^2} \frac{\alpha}{\pi} N_C Q_f^2 \, 2 f_{H\gamma}(x_{fH}), \tag{11}$$

$$a_{\mu;\text{f-rest,HZ}}^{\text{EW(2)}}(f) = \frac{G_F}{\sqrt{2}} \frac{m_\mu^2}{8\pi^2} \frac{\alpha}{\pi} N_C Q_f \frac{I_f^3 - 2s_W^2 Q_f}{4c_W^2 s_W^2} (1 - 4s_W^2) \, f_{HZ}(x_{fH}, x_{fZ}), \tag{12}$$

with $x_{fH} = m_f^2/M_H^2$ and $x_{fZ} = m_f^2/M_Z^2$. The loop functions can be written in terms of one-dimensional integral representations or in terms of dilogarithms:

$$f_{H\gamma}(x) = \int_0^1 dw \, x \frac{2w^2 - 2w + 1}{w^2 - w + x} \log \frac{w(1-w)}{x} \tag{13}$$

$$= x \left[f_{\text{H}}(x) - 4 \right], \tag{14}$$

$$f_{HZ}(x, z) = \int_0^1 dw \, x \, z \frac{2w^2 - 2w + 1}{w^2 - w + z} \left[\frac{\log \frac{w(1-w)}{x}}{w^2 - w + x} + \frac{\log \frac{x}{z}}{x - z} \right] \tag{15}$$

$$= \frac{x \, z}{x - z} \left[f_{\text{H}}(z) - f_{\text{H}}(x) \right]. \tag{16}$$

The dilogarithms are contained in the function $f_{\text{H}}(x)$, defined as[2]

$$f_{\text{H}}(x) = \frac{4x - 2}{y} \left[\text{Li}_2 \left(1 - \frac{1-y}{2x} \right) - \text{Li}_2 \left(1 - \frac{1+y}{2x} \right) \right] - 2 \log x, \tag{17}$$

with $y = \sqrt{1 - 4x}$. Further, the weak isospin I_f^3 is defined as $\pm\frac{1}{2}$ for up (down) fermions, and the electric charge Q_f equals $+\frac{2}{3}, -\frac{1}{3}, -1$ for up-type quarks, down-type quarks and charged leptons, respectively. The color factor N_C is 1 for leptons and 3 for quarks.

Fig. 3(a) shows the numerical result as a function of the Higgs boson mass and compares with the numerical values obtained in Ref. [21], using their approximations. We find that the approximation for large M_H is surprisingly poor. As a check of this case, we have explicitly computed the higher orders in the expansion in m_t^2/M_H^2 and verified that the terms neglected in Ref. [21] are important.

Inserting the measured value of the Higgs boson mass, and taking into account all contributions including top, bottom, charm and τ loops and diagrams

---

[2] In Ref. [26], Eq.(70), a similar function $f_S(x)$ is defined, where $f_S(x) = x f_{\text{H}}(x) - 4x$. Additionally, Eqs. (14), (16) are connected by $f_{H\gamma}(x) = \lim_{z \to \infty} f_{HZ}(x, z)$.
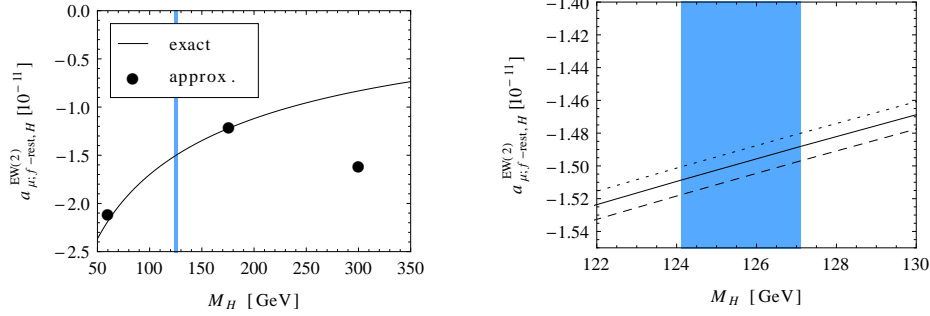
Figure 3: Numerical result for $a_{\mu;\text{f-rest,H}}^{\text{EW}(2)}$ as a function of the Higgs boson mass. The vertical band indicates the measured value of M_H. The fat dots in the left plot correspond to the approximations for $M_H = 60$ GeV, m_t, 300 GeV given in Ref. [21]. In the right plot the dotted, solid, dashed lines correspond to a variation of m_t by $(-1.4, 0, +1.4)$ GeV, respectively.

with Higgs and Z-boson exchange, we obtain

$$a_{\mu;\text{f-rest,H}}^{\text{EW}(2)} = (-1.50 \pm 0.01) \times 10^{-11}, \tag{18}$$

where the indicated error arises essentially from the uncertainty of the input parameters m_t and M_H. Again, the result is in agreement with the intervals given in Refs. [4,5,21], which differ because of the different allowed Higgs boson mass ranges.

Eqs. (8), (11)–(18) and Figs. 2 and 3 constitute our main new results. In the following we briefly review the remaining electroweak contributions, with slight updates.

The non-Higgs dependent contributions $a_{\mu;\text{f-rest,no H}}^{\text{EW}(2)}$ are given by:

$$\begin{aligned}
a_{\mu;\text{f-rest,no H}}^{\text{EW}(2)} = & -\frac{G_F}{\sqrt{2}} \frac{m_\mu^2}{8\pi^2} \frac{\alpha}{\pi} \left[\frac{1}{2s_W^2} \left(\frac{5}{8} \frac{m_t^2}{M_W^2} + \log \frac{m_t^2}{M_W^2} + \frac{7}{3} \right) \right] \\
& -\frac{G_F}{\sqrt{2}} \frac{m_\mu^2}{8\pi^2} \frac{\alpha}{\pi} \left[\frac{c_W^2}{2s_W^2} \frac{m_t^2}{M_W^2} \left(1 - 4s_W^2 \right) \right] \\
& -\frac{G_F}{\sqrt{2}} \frac{m_\mu^2}{8\pi^2} \frac{\alpha}{\pi} \left[\left(\frac{8}{9} \log \frac{M_Z}{m_\mu} + \frac{4}{9} \log \frac{M_Z}{m_\tau} \right) \left(1 - 4s_W^2 \right)^2 \right. \\
& \left. + \frac{4}{3} \times 6.88 \left(1 - 4s_W^2 \right) \right].
\end{aligned} \tag{19}$$

The first line has been computed in Ref. [21] and was re-written in this form e.g. in Ref. [4, 27]; the other two terms correspond to additional terms added in Ref. [14], where however no explicit formula was provided. These terms are suppressed by $(1-4s_W^2)$ but enhanced by either m_t^2/M_W^2 or by large logarithms. The factor m_t^2/M_W^2 enters via the quantity $\Delta\rho$, which arises by applying the renormalization $s_W^2 \rightarrow s_W^2 + \delta s_W^2$ in the $(1 - 4s_W^2)^2$-term of the one-loop result (7). The other term originates from diagrams with γ–Z mixing as shown
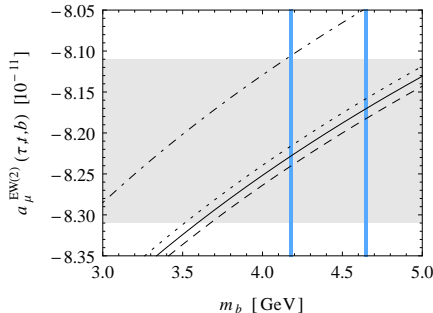
6

Figure 4: Numerical result for $a_\mu^{\mathrm{EW}(2)}(\tau, t, b)$ as a function of the bottom quark mass, for various values of the top quark mass. The dash-dotted line corresponds to the $\overline{\mathrm{MS}}$ mass $\overline{m}_t = 160$ GeV; the solid, dotted, dashed lines to the pole mass $m_t = 173.5$ GeV and variations thereof by ∓ 1.4 GeV. The vertical blue lines indicate the values of $\overline{\mathrm{MS}}$ mass $\overline{m}_b(\overline{m}_b) = 4.18$ GeV and the 1S-mass 4.65 GeV [17]; the $\overline{\mathrm{MS}}$ mass at higher scales has smaller values. The horizontal gray band corresponds to the result (21).

in Fig. 1(d) with light fermions running in the loop. It can be computed using renormalization-group techniques [14, 28]. The number 6.88 in the last line has been obtained in Ref. [14] as a nonperturbative replacement of the perturbative expression $2/3 \sum_{q=u,d,s,c,b} N_c \left(I_q^3 Q_q - 2Q_q^2 s_W^2 \right) \log M_Z / m_q$. Numerically, we obtain $-4.12, -0.24, -0.29$ in units of 10^{-11} for the three contributions, in total

$$a_{\mu;\mathrm{f\text{-}rest,no\ H}}^{\mathrm{EW}(2)} = (-4.65 \pm 0.10) \times 10^{-11}. \tag{20}$$

The error due to the uncertainty of the input parameters is negligible; the given error is our estimate of the still neglected terms which are suppressed by a factor $(1 - 4s_W^2)$ or M_Z^2 / m_t^2 and not enhanced by anything. The estimate is obtained by comparison with the computed terms in the second and third line of Eq. (19) and the respective enhancement factors.

For the third generation contributions to Fig. 1(c) perturbation theory can be applied, and these contributions have been evaluated in Refs. [14, 21, 29]. The result and the error estimate from Ref. [14], including subleading terms in m_t^2 / M_Z^2, read

$$a_\mu^{\mathrm{EW}(2)}(\tau, t, b) = -(8.21 \pm 0.10) \times 10^{-11}. \tag{21}$$

We have re-evaluated these contributions for various definitions of quark masses which differ by higher orders in the strong interaction, similarly to the error estimation by Ref. [14]. The result is shown in Fig. 4, and it confirms that Eq. (21) is still compatible with present values of quark masses.

The contribution of the first two generations to Fig. 1(c) has first been fully computed in Ref. [21], approximating the light quark contributions by a naive

perturbative calculation with constituent-like quark masses. The light quark contributions have been treated in a more satisfactory way in Refs. [14, 29, 30]. The final result of Ref. [14] is[3]

$$a_\mu^{\mathrm{EW}(2)}(e, \mu, u, c, d, s) = -(6.91 \pm 0.20 \pm 0.30) \times 10^{-11}, \qquad (22)$$

where the uncertainties for the 1st and 2nd generation have been given separately.

Contributions from beyond the two-loop level have been considered in Refs. [14, 28]. There, the leading logarithms at the three-loop level have been obtained from renormalization-group methods. It was found that these logarithms amount to 0.4×10^{-11}, if the two-loop result is parametrized in terms of $G_F \, \alpha(m_\mu)$, where $\alpha(m_\mu)$ is the running fine-structure constant at the scale of the muon mass. If the two-loop result is parametrized in terms of $G_F \, \alpha$, however, the shift of the coupling accidentally cancels the three-loop logarithms. Hence, since this is the parametrization we have used, we take

$$a_\mu^{\mathrm{EW}(\geq 3)} = (0 \pm 0.20) \times 10^{-11}, \qquad (23)$$

where the error estimate is from Ref. [14]. It corresponds to estimating the non-leading logarithmic three-loop contributions to be below a percent of the two-loop contributions.

In summary, we have re-evaluated the electroweak contributions to a_μ using the measured Higgs boson mass and employing consistently the $G_F \, \alpha$ parametrization at the two-loop level. We provide exact numerical results for the full bosonic and the Higgs-dependent fermionic two-loop contributions, for the latter also analytical results. These results are supplemented by updates of the most advanced available results on all other electroweak contributions. Our final result obtained from Eqs. (7), (8), (18), (20), (21), (22), (23) reads

$$a_\mu^{\mathrm{EW}} = (153.6 \pm 1.0) \times 10^{-11}. \qquad (24)$$

We assess the final theory error of these contributions to be $\pm 1.0 \times 10^{-11}$. This is the same value as the one given in Ref. [14] for the overall hadronic uncertainty from the diagrams of Fig. 1(c), which is now by far the dominant source of error of the electroweak contributions. The error from unknown three-loop contributions and neglected two-loop terms suppressed by M_Z^2/m_t^2 and $(1-4s_W^2)$ is significantly smaller and the error due to the experimental uncertainty of the Higgs boson, W-boson, and top-quark mass is well below 10^{-12} and thus negligible.

Our result can be compared with the QED contributions. In units of 10^{-12}, our result shifts the electroweak contributions by $+4$ (compared to Ref. [4]), $+6$ (to Ref. [5]), and -4 (to Ref. [14]). In contrast, the recent 5-loop calculation [6] has shifted the QED result by $+8$. Combining these new results with

---

[3]The result is taken from the erratum of Ref. [14]. It is perfectly compatible with the one provided in Ref. [4]. The result quoted in Ref. [5] was taken from the original Ref. [14]; it differs slightly but is also compatible within the errors.

the two recent evaluations of the hadronic contributions [7, 8], we obtain the following differences between the measurement Eq. (1) and the full Standard Model prediction:

$$a_\mu^{\exp} - a_\mu^{\mathrm{SM}} = \begin{cases} (286 \pm 80) \times 10^{-11} & [7], \\ (261 \pm 80) \times 10^{-11} & [8]. \end{cases} \tag{25}$$

The Standard Model theory error remains dominated by the non-electroweak hadronic contributions. The QED and electroweak contributions can now be regarded as sufficiently accurate for the precision of next generation experiments.

Acknowledgements

References

[1] G.W. Bennett, et al., (Muon $(g-2)$ Collaboration), Phys. Rev. D **73**, 072003 (2006).

[2] D. W. Hertzog, B. Lee Roberts et al., Fermilab Proposal P-989, March 2009, `http://www.fnal.gov/directorate/program_planning/ Mar2009PACPublic/PACMarch09AgendaPublic.htm`; B. L. Roberts, arXiv:1001.2898 [hep-ex].

[3] H. Iinuma [J-PARC New g-2/EDM experiment Collaboration], J. Phys. Conf. Ser. **295** (2011) 012032.

[4] F. Jegerlehner and A. Nyffeler, Phys. Rept. **477** (2009) 1.

[5] J. Miller, E. de Rafael, B.L. Roberts, D. Stöckinger, Ann.Rev.Nucl.Part. (2012) 62.

[6] T. Aoyama, M. Hayakawa, T. Kinoshita and M. Nio, Phys. Rev. Lett. **109** (2012) 111808 [arXiv:1205.5370 [hep-ph]].

[7] M. Davier, A. Hoecker, B. Malaescu and Z. Zhang, Eur. Phys. J. C **71** (2011) 1515 [Erratum-ibid. C **72** (2012) 1874] [arXiv:1010.4180 [hep-ph]].

[8] K. Hagiwara, R. Liao, A. D. Martin, D. Nomura and T. Teubner, J. Phys. G G **38** (2011) 085003 [arXiv:1105.3149 [hep-ph]].

[9] M. Benayoun, P. David, L. DelBuono and F. Jegerlehner, arXiv:1210.7184 [hep-ph].

[10] F. Jegerlehner and R. Szafron, Eur. Phys. J. C **71** (2011) 1632 [arXiv:1101.2872 [hep-ph]].

[11] J. Prades, E. de Rafael and A. Vainshtein, arXiv:0901.0306 [hep-ph].

[12] T. Goecke, C. S. Fischer and R. Williams, Phys. Rev. D **83** (2011) 094006 [Erratum-ibid. D **86** (2012) 099901] [arXiv:1012.3886 [hep-ph]].

[13] T. Blum, M. Hayakawa and T. Izubuchi, arXiv:1301.2607[hep-ph].

[14] A. Czarnecki, W. J. Marciano, A. Vainshtein Phys.Rev.D **67** (2003) 073006, Erratum-ibid.D**73** (2006) 119901.

[15] [ATLAS Collaboration], ATLAS-CONF-2013-014.

[16] [CMS Collaboration], CMS-PAS-HIG-13-005.

[17] J. Beringer et al. (Particle Data Group) Phys. Rev. D **86** (2012) 010001.

[18] A. Czarnecki, B. Krause and W. J. Marciano, Phys. Rev. Lett. **76** (1996) 3267 [hep-ph/9512369].

[19] S. Heinemeyer, D. Stöckinger and G. Weiglein, Nucl. Phys. B **699** (2004) 103.

[20] T. Gribouk and A. Czarnecki, Phys. Rev. D **72** (2005) 053016 [hep-ph/0509205].

[21] A. Czarnecki, B. Krause and W. J. Marciano, Phys. Rev. D **52** (1995) 2619

[22] K. -m. Cheung, C. -H. Chou and O. C. W. Kong, Phys. Rev. D **64** (2001) 111301 [hep-ph/0103183].

[23] Y. -L. Wu and Y. -F. Zhou, Phys. Rev. D **64** (2001) 115018 [hep-ph/0104056].

[24] S. Heinemeyer, D. Stöckinger and G. Weiglein, Nucl. Phys. B **690** (2004) 62.

[25] S. M. Barr and A. Zee, "Electric Dipole Moment Of The Electron And Of The Neutron," Phys. Rev. Lett. **65** (1990) 21 [Erratum-ibid. **65** (1990) 2920].

[26] D. Stöckinger, "The Muon Magnetic Moment and Supersymmetry," J. Phys. G**34** (2006) R45-R92.

[27] M. Knecht, Lect. Notes Phys. **629** (2004) 37-84

[28] G. Degrassi and G. F. Giudice, Phys. Rev. D **58** (1998) 053007.

[29] S. Peris, M. Perrottet and E. de Rafael, Phys. Lett. B **355** (1995) 523 [hep-ph/9505405].

[30] M. Knecht, S. Peris, M. Perrottet and E. De Rafael, JHEP **0211** (2002) 003 [hep-ph/0205102].